Supporting Information

Sjölund et al. 10.1073/pnas.1322275111

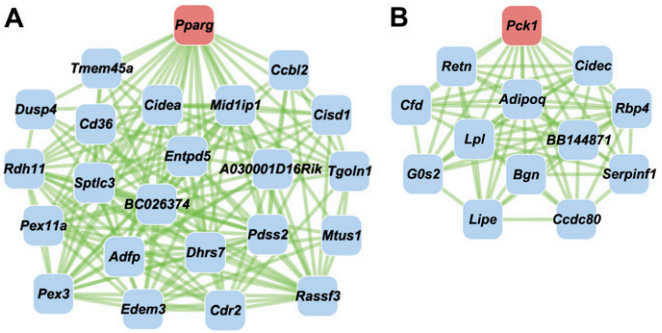

Fig. S1. Skin gene networks of *Pparg* and *Pck1*. (*A*) Peroxisome proliferative activated receptor gamma, coactivator 1 alpha (*Pparg*) (red) correlation subnetwork (rho > ±0.70) in *Mus spretus*/*Mus musculus* backcross mice (FVBBX) epidermis. (*B*) *Pck1* (red) correlation subnetwork (rho ≥ ±0.65) in FVBBX epidermis.

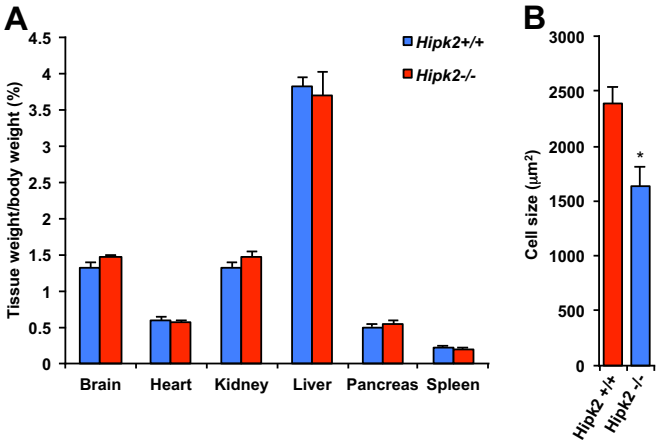

Fig. S2. (*A*) Weights of the brain, heart, kidney, liver, pancreas, and spleen remain essentially unchanged in *homeodomain-interacting protein kinase 2* (*Hipk2*) knockout mice compared with *Hipk2* wild-type mice. Weights of the indicated tissues from 8-wk-old female $Hipk2^{+/+}$ ($n = 8$) and $Hipk2^{-/-}$ ($n = 8$) mice after normalization to body weight. Data are presented as mean ± SEM. (*B*) Adipocyte cell size is significantly reduced in *Hipk2* knockout mice compared with *Hipk2* wild-type mice. Adipocyte size of ovarian white adipose tissue from 8- to 10-wk-old female $Hipk2^{+/+}$ ($n = 4$) and $Hipk2^{-/-}$ mice ($n = 4$). *$P < 0.05$ for $Hipk2^{+/+}$ versus $Hipk2^{-/-}$ mice. Data are presented as mean ± SEM.

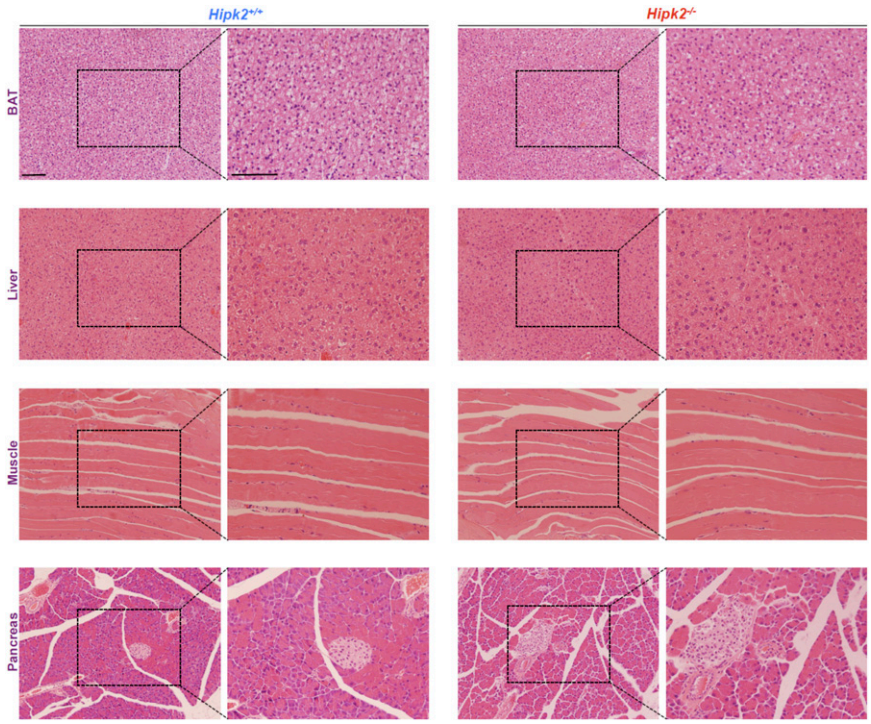

Fig. S3. *Hipk2* knockout mice have unaltered brown adipose tissue (BAT), liver, skeletal muscle, and pancreas morphology. Representative images of the indicated tissues from *Hipk2*$^{+/+}$ and *Hipk2*$^{-/-}$ mice stained with H&E. (Scale bars, 100 μm.)

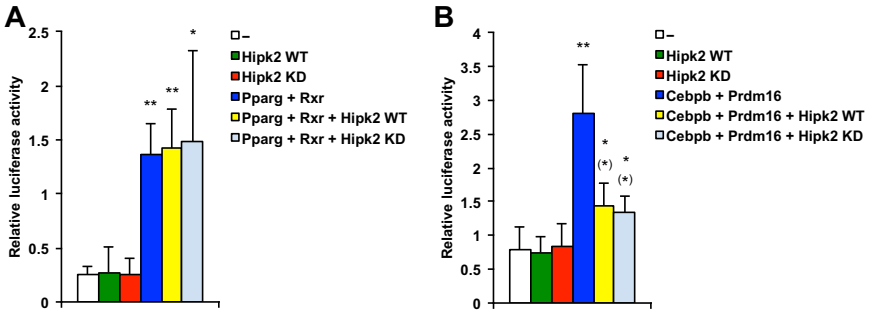

Fig. S4. Hipk2 represses *Ppargc1a* transcription. (*A*) Relative luciferase activity in extracts from 3T3-L1 cells transfected with the *PPRE-Luc* reporter construct, *Hipk2* WT, *Hipk2* kinase-dead (KD), *Pparg*, and/or *Rxra* expression vectors ($n = 3$). (*B*) Relative luciferase activity in extracts from 3T3-L1 cells transfected with the *Ppargc1a-Luc* reporter construct, *Hipk2* WT, *Hipk2* KD, *Cebpb*, and/or *Prdm16* expression vectors ($n = 3$). *$P < 0.05$ and **$P < 0.01$ for expression vectors versus control (–) and $^{(*)}P < 0.05$ for *Hipk2* WT/KD versus *Cebpb* + *Prdm16*. Data are presented as mean ± SEM.

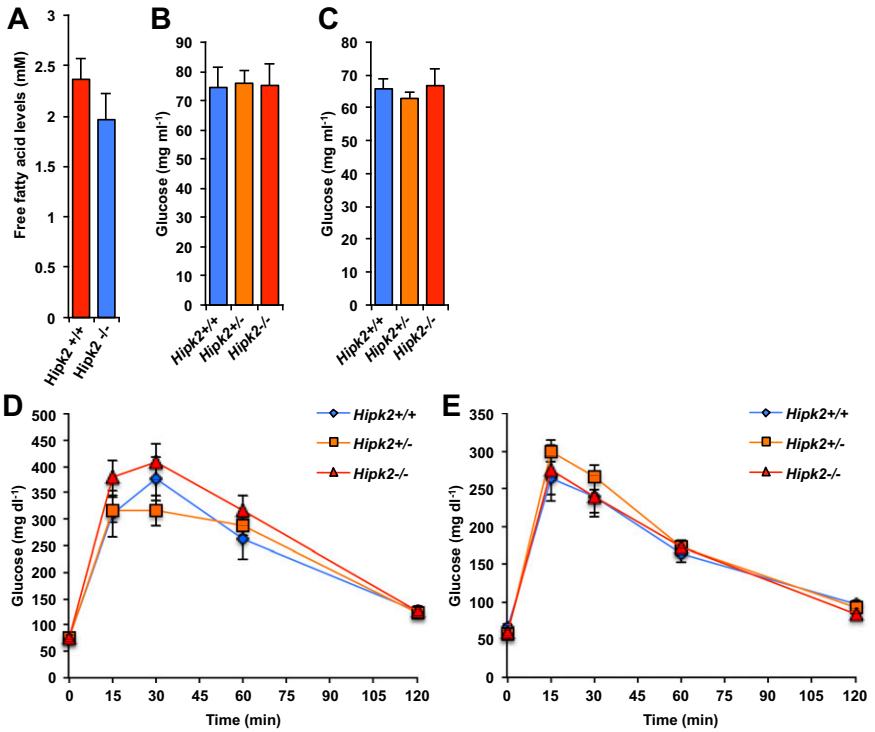

Fig. S5. Free fatty acid levels, glucose levels, and glucose clearance in *Hipk2*-null mice are comparable to wild-type littermates. (*A*) Free fatty acid concentrations were determined in fasted (6 h) female $Hipk2^{+/+}$ ($n = 3$) and $Hipk2^{-/-}$ ($n = 6$) mice. (*B* and *C*) Blood glucose levels of male (*B*) and female (*C*) $Hipk2^{+/+}$, $Hipk2^{+/-}$, and $Hipk2^{-/-}$ mice ($n = 7$–14, $Hipk2^{+/+}$; $n = 14$–16, $Hipk2^{+/-}$; $n = 7$–10, $Hipk2^{-/-}$). (*D* and *E*) Glucose tolerance tests on male (*D*) and female (*E*) $Hipk2^{+/+}$, $Hipk2^{+/-}$, and $Hipk2^{-/-}$ mice ($n = 6$–14, $Hipk2^{+/+}$; $n = 17$, $Hipk2^{+/-}$; $n = 6$–8, $Hipk2^{-/-}$). Data are presented as mean ± SEM.

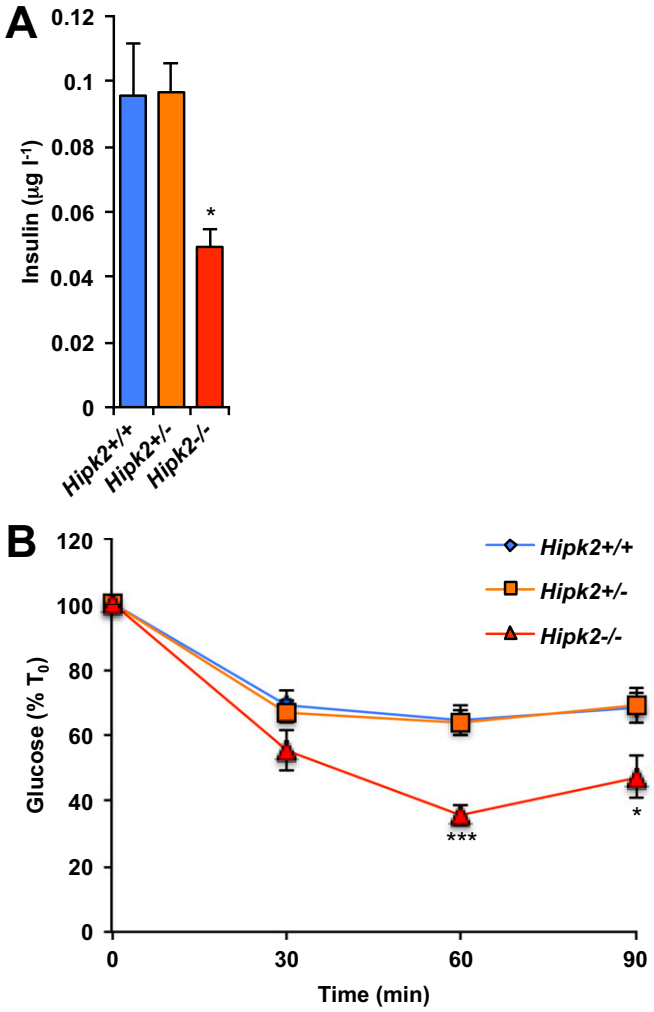

Fig. S6. Loss of *Hipk2* reduces basal insulin levels and increases insulin sensitivity. (*A*) Plasma insulin levels of 8- to 10-wk-old male $Hipk2^{+/+}$, $Hipk2^{+/-}$, and $Hipk2^{-/-}$ mice ($n = 7$, $Hipk2^{+/+}$; $n = 14$, $Hipk2^{+/-}$; $n = 7$, $Hipk2^{-/-}$). (*B*) Insulin tolerance tests on 8- to 10-wk-old male $Hipk2^{+/+}$, $Hipk2^{+/-}$, and $Hipk2^{-/-}$ mice ($n = 6$, $Hipk2^{+/+}$; $n = 17$, $Hipk2^{+/-}$; $n = 6$, $Hipk2^{-/-}$). T_0, time zero (start of the experiment, i.e., the basal level when insulin was injected). $^*P < 0.05$ and $^{***}P < 0.001$ for $Hipk2^{+/+}$ versus $Hipk2^{+/-}$ or $Hipk2^{-/-}$ mice. Data are presented as mean ± SEM.

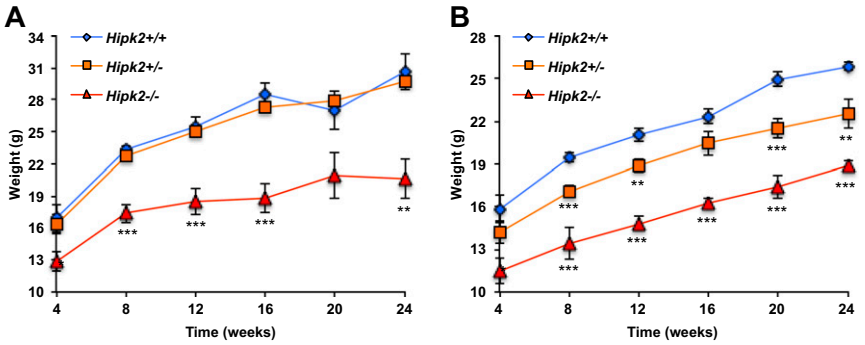

Fig. S7. *Hipk2* knockout mice weigh less than control group littermates. Body weights of male (*A*) and female (*B*) $Hipk2^{+/+}$, $Hipk2^{+/-}$, and $Hipk2^{-/-}$ mice ($n =$ 12–26, $Hipk2^{+/+}$; $n =$ 8–30, $Hipk2^{+/-}$; $n =$ 6–17, $Hipk2^{-/-}$). $^*P < 0.05$, $^{**}P < 0.01$, and $^{***}P < 0.001$ for $Hipk2^{+/+}$ versus $Hipk2^{+/-}$ or $Hipk2^{-/-}$ mice. Data are presented as mean ± SEM.

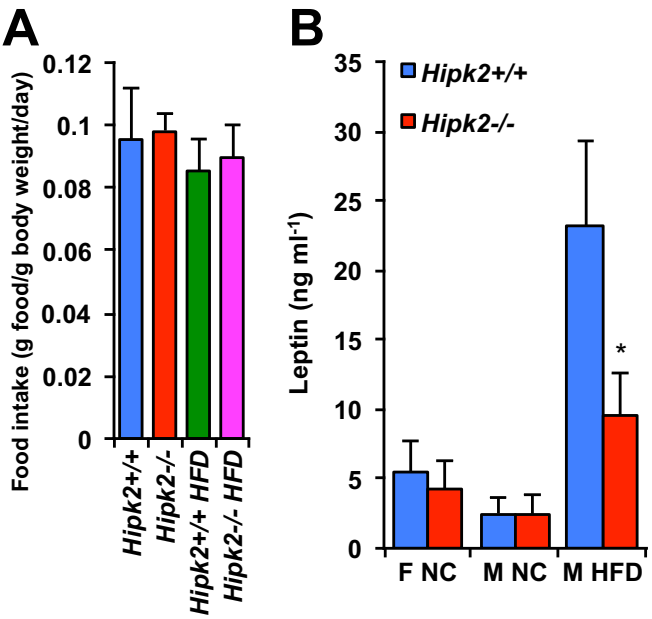

Fig. S8. (*A*) Food intake is indistinguishable between *Hipk2*-null mice and Hipk2 wild-type mice. Daily food intake normalized to body weight of $Hipk2^{+/+}$ ($n = 7$) and $Hipk2^{-/-}$ ($n = 7$) mice on normal chow or a high-fat diet (HFD). Data are presented as mean ± SEM. (*B*) There are significantly lower circulating levels of leptin in male *Hipk2*-null mice compared with Hipk2 WT mice on a high-fat diet. Plasma leptin levels in normal chow-fed (NC) female (F) and male (M) mice or HFD-fed male mice ($n = 4$–8). *$P < 0.05$ for $Hipk2^{+/+}$ versus $Hipk2^{-/-}$ mice. Data are presented as mean ± SEM.

Table S1. Hipk2 correlations to adipocyte-associated genes are more pronounced in female mice

Top 40 Hipk2 correlations in female FVBBX mice	rho	Top 40 Hipk2 correlations in male FVBBX mice	rho
Scd1	0.81	*Hoxd10*	0.76
Rassf3	0.80	*Gse1*	0.76
A030001D16Rik	0.80	*Rab3ip*	0.76
Fa2h	0.80	*Tpm1*	0.76
Ptplb	0.79	*Palld*	0.76
Mid1ip1	0.79	***Elovl4***	0.75
Pank1	0.77	*Tmem62*	0.75
Mgll	0.77	***Far2***	0.74
3110001I20Rik	0.77	*AI646023*	0.74
Crat	0.76	*Tmem139*	0.73
Dhcr24	0.76	*Pdzrn3*	0.73
Soat1	0.76	*D630004K10Rik*	0.73
2610019F03Rik	0.76	*Col4a5*	0.73
Far2	0.75	*Mark1*	0.72
Pxmp4	0.75	*Enc1*	0.72
Gnmt	0.75	*Rassf3*	0.71
Hsd3b2	0.74	*Gpr125*	0.71
Pdss2	0.73	*Lbh*	0.71
Dock3	0.73	*E430014L09Rik*	0.71
Mgst1	0.73	*Frmd4a*	0.71
Acot1	0.73	*Sardh*	0.71
Arl6ip2	0.73	*Cpe*	0.70
2310001A20Rik	0.73	*Nfe2l3*	0.70
Edem3	0.72	*Gli1*	0.70
Pparg	0.72	*Marcksl1*	0.70
2010305C02Rik	0.72	*Nrp2*	0.70
Brp44	0.72	*1200009O22Rik*	0.69
Leng4	0.72	*Krtap3-3*	0.69
Zcd1	0.72	*Slc39a10*	0.69
Slc27a1	0.72	*Pcp4*	0.69
Hoxb2	0.71	***Acsm3***	0.69
Elovl4	0.71	*BC024479*	0.69
1200015F23Rik	0.71	*Odz3*	0.68
Cat	0.71	*Sh3d19*	0.68
Pnpla5	0.71	*Echdc1*	0.68
Tmem164	0.71	*2610019P18Rik*	0.68
Acsm3	0.71	*9130213B05Rik*	0.68
Panx3	0.71	*Scrg1*	0.68
Ccbl2	0.71	*Pitrm1*	0.67
Ppa1	0.71	*Hnrpa2b1*	0.67

Hipk2 correlations in epidermis from female ($n = 40$) and male ($n = 31$) FVBBX mice. Genes in bold are directly annotated to the Gene Ontology (GO) term "lipid metabolic process" (GO ID code 0006629).

Table S2. TaqMan probes used for quantitative PCR analysis

Gene	TaqMan probe
Adfp	Mm00475794_m1
Adipoq	Mm00456425_m1
Cebpa	Mm00514283_s1
Cebpb	Mm00843434_s1
CD36	Mm01135198_m1
Cfd	Mm01143935_g1
Cidea	Mm00432554_m1
Fabp4	Mm00445878_m1
Fa2h	Mm00626259_m1
Hipk2	Mm00439329_m1
Mest	Mm00484993_m1
Lipe	Mm00495359_m1
Pank1	Mm00458408_m1
Pck1	Mm01247058_m1
Pparg1/2	Mm00440945_m1
Pparg2	Mm00440940_m1
Ppargc1a	Mm01208835_m1
Rbp4	Mm00803264_g1
Scd1	Mm00772290_m1
Ucp1	Mm0494069_m1